Inorg. Chem. **2007**, *46*, 8577–8583

Hydrogen Bonding and Multiphonon Structure in Copper Pyrazine Coordination Polymers

S. Brown,[†,⊥] J. Cao,[†] J. L. Musfeldt,*[,†] M. M. Conner,[‡] A. C. McConnell,[‡] H. I. Southerland,[‡] J. L. Manson,[‡] J. A. Schlueter,[§] M. D. Phillips,[||] M. M. Turnbull,[||] and C. P. Landee[||]

Department of Chemistry, University of Tennessee, Knoxville, Tennessee 37996, Department of Chemistry and Biochemistry, Eastern Washington University, Cheney, Washington 99004, Materials Science Division, Argonne National Laboratory, Argonne, Illinois 60439, and Department of Physics and Carlson School of Chemistry, Clark University, Worcester, Massachusetts 01477

Received January 24, 2007

We report a systematic investigation of the temperature-dependent infrared vibrational spectra of a family of chemically related coordination polymer magnets based upon bridging bifluoride (HF_2^-) and terminal fluoride (F^-) ligands in copper pyrazine complexes including $Cu(HF_2)(pyz)_2BF_4$, $Cu(HF_2)(pyz)_2ClO_4$, and $CuF_2(H_2O)_2(pyz)$. We compare our results with several one- and two-dimensional prototype materials including $Cu(pyz)(NO_3)_2$ and $Cu(pyz)_2(ClO_4)_2$. Unusual low-temperature hydrogen bonding, local structural transitions associated with stronger low-temperature hydrogen bonding, and striking multiphonon effects that derive from coupling of an infrared-active fundamental with strong Raman-active modes of the pyrazine building-block molecule are observed. On the basis of the spectroscopic evidence, these interactions are ubiquitous to this family of coordination polymers and may work to stabilize long-range magnetic ordering at low temperature. Similar interactions are likely to be present in other molecule-based magnets.

I. Introduction

The finding that hydrogen bonding can control both long-range and local structure while providing significant magnetic exchange pathways has attracted considerable attention, renewing interest in tunable families of low-dimensional solids such as polymeric magnets and related compounds.[1−21] At the same time, these materials are useful for investigating fundamental predictions of quantum magnetism because they are physical manifestations of one- and two-dimensional (1D and 2D) magnets.[22−24] In order to test the ability of hydrogen-bonding interactions to create three-dimensional (3D) networks, it is desirable to prepare complexes with chemically flexible building-block units (such as pyrazine, which ligates easily with various paramagnetic metal ions) and ligands that can engage in very strong hydrogen-bonding interactions.

* To whom correspondence should be addressed. E-mail: musfeldt@utk.edu.
[⊥] Present address: University College of London.
[†] University of Tennessee.
[‡] Eastern Washington University.
[§] Argonne National Laboratory.
[||] Clark University.

(1) Manson, J. L.; Conner, M. M.; Schlueter, J. A.; Lancaster, T.; Blundell, S. J.; Brooks, M. L.; Pratt, F. L.; Papageorgiou, T.; Bianchi, A. D.; Wosnitza, J.; Whangbo, M. H. *Chem. Commun.* **2006**, 4894.
(2) Conner, M.; McConnell, A.; Schlueter, J.; Manson, J. *J. Low Temp. Phys.* **2006**, *142*, 273.
(3) Orendacova, A.; Kajnakova, M.; Cernak, J.; Park, J. H.; Cizmar, E.; Orendac, M.; Vlcek, A.; Kravchyna, O. V.; Anders, A. G.; Feher, A.; Meisel, M. W. *Chem. Phys.* **2005**, *309*, 115.
(4) Kajnakova, M.; Orendac, M.; Orendacova, A.; Vlcek, A.; Cernak, J.; Kravchyna, O. V.; Anders, A. G.; Balanda, M.; Park, J. H.; Feher, A.; Meisel, M. W. *Phys. Rev. B* **2005**, *71*, 014435.
(5) Ferrer, J. R.; Lahti, P. M.; George, C.; Oliete, P.; Julier, M.; Palacio, F. *Chem. Mater.* **2001**, *13*, 2447.
(6) Field, L.; Lahti, P. M. *Chem. Mater.* **2003**, *15*, 2861.
(7) Oeretel, C. M.; Sweeder, R. D.; Patel, S.; Downie, C. M.; DiSalvo, F. J. *Inorg. Chem.* **2005**, *44*, 2287.
(8) Krishnamohan Sharma, C. V.; Chusuei, C. C.; Clérac, R.; Möller, T.; Dunbar, K. R.; Clearfield, A. *Inorg. Chem.* **2003**, *42*, 8300.
(9) Mitzi, D. *Inorg. Chem.* **2005**, *44*, 3755.
(10) Toma, L.; Toma, L. M.; Lescouëzec, R.; Armentano, D.; De Munno, G.; Andruh, M.; Cano, J.; Lloret, F.; Julve, M. *Dalton Trans.* **2005**, 1357.
(11) Baudron, S. A.; Batail, P.; Coulon, C.; Clérac, R.; Canadell, E.; Laukhin, V.; Melzi, R.; Wzietek, P.; Jérome, D.; Auban-Senzier, P.; Ravy, S. *J. Am. Chem. Soc.* **2005**, *127*, 11785.
(12) Cao, J.; Haraldsen, J. T.; Brown, S.; Musfeldt, J. L.; Thompson, J. R.; Zvyagin, S.; Krzystek, J.; Whangbo, M. H.; Nagler, S. E.; Torardi, C. C. *Phys. Rev. B* **2005**, *72*, 214421.
(13) Katsufuji, T.; Takagi, H. *Phys. Rev. B* **2004**, *69*, 064422.
(14) Caputo, R. E.; Willett, R. D. *Phys. Rev. B* **1976**, *13*, 3956.
(15) Doyle, R. P.; Julve, M.; Lloret, R.; Nieuwenhuyzen, M.; Kruger, P. E. *Dalton Trans.* **2006**, 2081.
(16) Ward, M. D. *Chem. Commun.* **2005**, 5838.

10.1021/ic070122t CCC: $37.00
Published on Web 09/11/2007

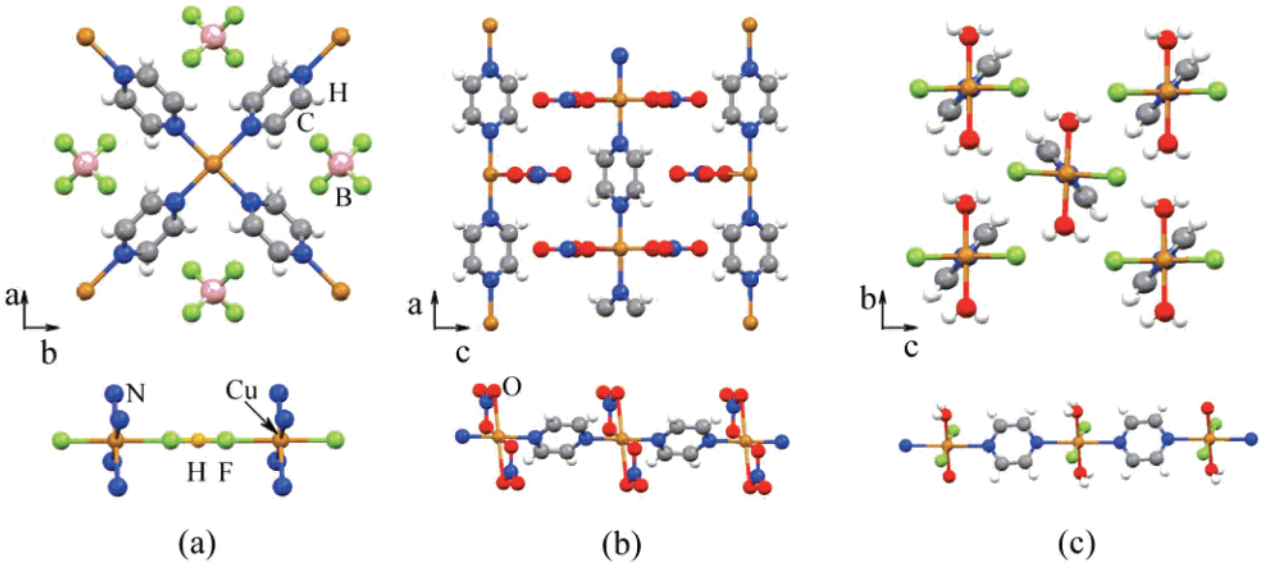

Figure 1. (a) Crystal structure of 2D $Cu(HF_2)(pyz)_2BF_4$ in the *ab* plane and a close-up view of bifluoride bridges between Cu centers along the *c* axis. (b) *Pmna* Crystal structure of 1D prototype $Cu(pyz)(NO_3)_2$ in the *ac* plane and a close-up view of the magnetic chain along the *a* axis.[27] (c) Crystal structure of 1D $CuF_2(H_2O)_2(pyz)$ in the *bc* plane and a close-up view of the magnetic chain along the *a* direction.

The bridging and terminal anions, bifluoride (HF_2^-) and fluoride (F^-), are unique in that they can be exploited to create new structure types with interesting properties. In the compounds of interest, $Cu(HF_2)(pyz)_2BF_4$ and $CuF_2(H_2O)_2$-(pyz), these ligands form linear and bent exchange pathways, respectively. The HF_2^- bridge is unusual in that it contains a two-coordinate H center, and it displays the strongest known hydrogen bond.

The development of chemically related compounds has traditionally been key to establishing structure−property relationships in complex materials. Figure 1 summarizes the crystal structures of the three most important compounds in this work: $Cu(HF_2)(pyz)_2BF_4$, the 1D model material Cu-$(pyz)(NO_3)_2$, and $CuF_2(H_2O)_2(pyz)$. In $Cu(HF_2)(pyz)_2BF_4$, the structure (*P*4/*nbm*, D_{4h}^3) is based upon 2D $Cu(pyz)^{2+}$ sheets in the *ab* plane.[1,2] These sheets are connected along the *c* axis by linear bridging HF_2^- anions, forming an unprecedented 3D network. Note that the sheets are similar to those in the prototypical square $S = {}^1/_2$ molecular antiferromagnet $Cu(pyz)_2(ClO_4)_2$, although in this case, the ClO_4^- anions behave as terminal groups rather than bridging linkages.[25] The B atom (in the BF_4^- anion) occupies the body-centered position in $Cu(HF_2)(pyz)_2BF_4$. This material displays long-range ordering below 1.54 K.[1] $CuF_2(H_2O)_2(pyz)$ crystallizes in the monoclinic space group $P2_1/c$ (C_{2h}^5) and contains Cu−pyz−Cu chains that run along the *a* axis.[2] The chains are separated by H_2O and F^- units coordinated to the Cu sites. Recently, long-range ordering has been observed in this material as well.[26] The chains in $CuF_2(H_2O)_2(pyz)$ are similar to those found in the prototypical $S = {}^1/_2$ Heisenberg antiferromagnet $Cu(pyz)(NO_3)_2$.[27−29] Here, the nitrate groups separate and isolate the magnetic chains, yielding a material with one of the largest known magnetic anisotropies ($J_\perp/J_{||} \sim 10^{-4}$).

Considering the evidence for important hydrogen-bond-mediated exchange interactions in these complex magnetic materials, it is very important to probe these interactions in greater detail. Infrared spectroscopy is a sensitive, direct, and microscopic technique that is uniquely sensitive to small changes in local environments. It is well-suited for work on the low-dimensional polymeric magnets of interest here. In order to understand the role of bifluoride and fluoride bridging and terminal ligands in a family of chemically related polymeric magnets, we investigated the variable-temperature vibrational properties of $Cu(HF_2)(pyz)_2BF_4$, Cu-$(HF_2)(pyz)_2ClO_4$, and $CuF_2(H_2O)_2(pyz)$, comparing the results to similar work on the $Cu(pyz)(NO_3)_2$ and $Cu(pyz)_2$-$(ClO_4)_2$ model compounds. We find that, in $CuF_2(H_2O)_2(pyz)$, the F···H−O network strengthens at low temperature,

(17) Papoutsakis, D.; Kirkby, J. P.; Jackson, J. E.; Nocera, D. G. *Chem.—Eur. J.* **1999**, *5*, 1474.
(18) Haddad, S. F.; Willett, R. D.; Landee, C. P. *Inorg. Chim. Acta* **2001**, *316*, 94.
(19) Youm, K. T.; Woo, H. K.; Ko, J.; Jun, M. J. *Cryst. Eng. Commun.* **2007**, *9*, 30.
(20) Geiser, U.; Schlueter, J. A. *Chem. Rev.* **2004**, *104*, 5203.
(21) Jones, B. R.; Olejniczak, I.; Dong, J.; Pigos, J. M.; Zhu, Z. T.; Garlach, A. D.; Musfeldt, J. L.; Koo, H. J.; Whangbo, M. H.; Schlueter, J. A.; Ward, B. H.; Morales, E.; Kini, A. M.; Winter, R. W.; Mohtasham, J.; Gard, G. L. *Chem. Mater.* **2000**, *12*, 2490.
(22) Endoh, Y.; Shirane, G.; Birgeneau, R. J.; Richards, P. M.; Holt, S. L. *Phys. Rev. Lett.* **1974**, *32*, 170.
(23) Kmety, C. R.; Manson, J. L.; Huang, Q.; Lynn, J. W.; Erwin, R. W.; Miller, J. S.; Epsein, A. *J. Phys. Rev. B* **1999**, *60*, 60.
(24) Lake, B.; Tennant, D. A.; Frost, C. D.; Nagler, S. E. *Nat. Mater.* **2005**, *4*, 329.
(25) Choi, J.; Woodward, J. D.; Musfeldt, J. L.; Landee, C. P.; Turnbull, M. M. *Chem. Mater.* **2003**, *15*, 2797.
(26) Manson, J. L.; Conner, M. M.; Schlueter, J. A.; McConnell, A. C.; Southerland, H. I.; Malfant, I.; Lancaster, T.; Blundell, S. J.; Brooks, M. L.; Pratt, F. L. *Chem. Commun.* **2007**, in preparation.
(27) Santoro, A.; Mighell, A. D.; Reimann, C. W. *Acta Crystallogr.* **1970**, *B26*, 979.
(28) Jones, B. R.; Varughese, P. A.; Olejniczak, I.; Pigos, J. M.; Musfeldt, J. L.; Landee, C. P.; Turnbull, M. M.; Carr, G. L. *Chem. Mater.* **2001**, *13*, 2127.
(29) Hammar, P. R.; Stone, M. B.; Reich, D. H.; Broholm, C.; Gibson, P. J.; Turnbull, M. M.; Landee, C. P.; Oshikawa, M. *Phys. Rev. B* **1999**, *59*, 1008.

causing the H_2O bond angle to widen slightly. The situation is more complicated in $Cu(HF_2)(pyz)_2BF_4$, where dominant BF_4···pyz interactions and, to a much lesser extent, weak longer-range HF_2···pyz interactions drive two weak structural distortions. The many available model compounds also facilitate a detailed analysis of the high-frequency multiphonon structure, the activation mechanism of which involves coupling with strong Raman-active modes of appropriate symmetry that derive from pyrazine motion.

II. Methods

Single crystals of all materials were grown via solution chemistry techniques. $Cu(HF_2)(pyz)_2BF_4$ was grown by aqueous reaction of stoichiometric amounts of $Cu(BF_4)_2{\cdot}yH_2O$, NH_4HF_2, and pyrazine as reported in ref 1. $Cu(HF_2)(pyz)_2ClO_4$ was prepared in a similar manner by replacing $Cu(BF_4)_2{\cdot}yH_2O$ with $Cu(ClO_4)_2{\cdot}6H_2O$. These two phases were determined to be isostructural by single-crystal X-ray diffraction. At 298 K, the unit cell of $Cu(HF_2)(pyz)_2ClO_4$ was determined to be $a = b = 9.7054(6)$ Å, $c = 6.6894(9)$ Å, and $V = 630.11$ Å^3. $CuF_2(H_2O)_2(pyz)$ was also grown by aqueous reaction of stoichiometric amounts of $Cu(NO_3)_2{\cdot}3H_2O$, NH_4F, and pyrazine. X-ray-quality single crystals were obtained in good yield by slow evaporation of the solvent. Because fluoride ion is produced during the course of the chemical reaction, reactions were carried out in plasticware. A detailed analysis of the crystal structure will be published separately.[26] Needlelike dark-blue crystals of $Cu(pyz)(NO_3)_2$ were obtained by slow evaporation of aqueous copper nitrate trihydrate and pyrazine in a 1:1 ratio as detailed in refs 27−29.

The infrared transmittance measurements were performed using two different Fourier transform infrared spectrometers, a Bruker 113V and an Equinox 55 equipped with a microscope attachment, covering the frequency range from 30 to 5000 cm^{-1} with 0.5 cm^{-1} resolution. A helium-cooled bolometer detector was employed in the far-infrared for added sensitivity. For single-crystal samples, appropriate polarizers were used to separate responses in different directions. Even with the thinnest crystal, however, a number of vibrational bands were saturated. As a result, we carried out selected measurements on isotropic, pressed pellets, using paraffin or KCl as the matrix material, depending on the frequency range of interest. The low-temperature spectroscopies were carried out with a continuous-flow helium cryostat and temperature controller. Standard peak-fitting procedures were employed as needed.

The crystal structure of $Cu(HF_2)(pyz)_2BF_4$ at 200 K was determined by X-ray diffraction using a Siemens SMART single-crystal diffractometer equipped with a CCD-based area detector and a sealed-tube Mo Kα source (graphite monochromator). Detector frames were integrated using the *SAINT* program,[30] and intensities were corrected for absorption by Gaussian integration based on the measured crystal shape using the XPREP capability. Other systematic variations were corrected by the analysis of replicate reflections using the program *SADABS*.[31] The structures were solved by use of direct methods, while full-matrix least-squares refinement on F^2 (including all data) was performed, both using the program package *SHELXTL*.[32] The largest residual electron density peaks lie on the bifluoride H atom and on the Cu−F bond, 0.923 Å from the Cu atom. Their location is consistent with stacking faults resulting from a shifting of the unit cell by 0.5 along the *c* axis, with the residual electron peaks due to the Cu and F positions of a minority-defect component.

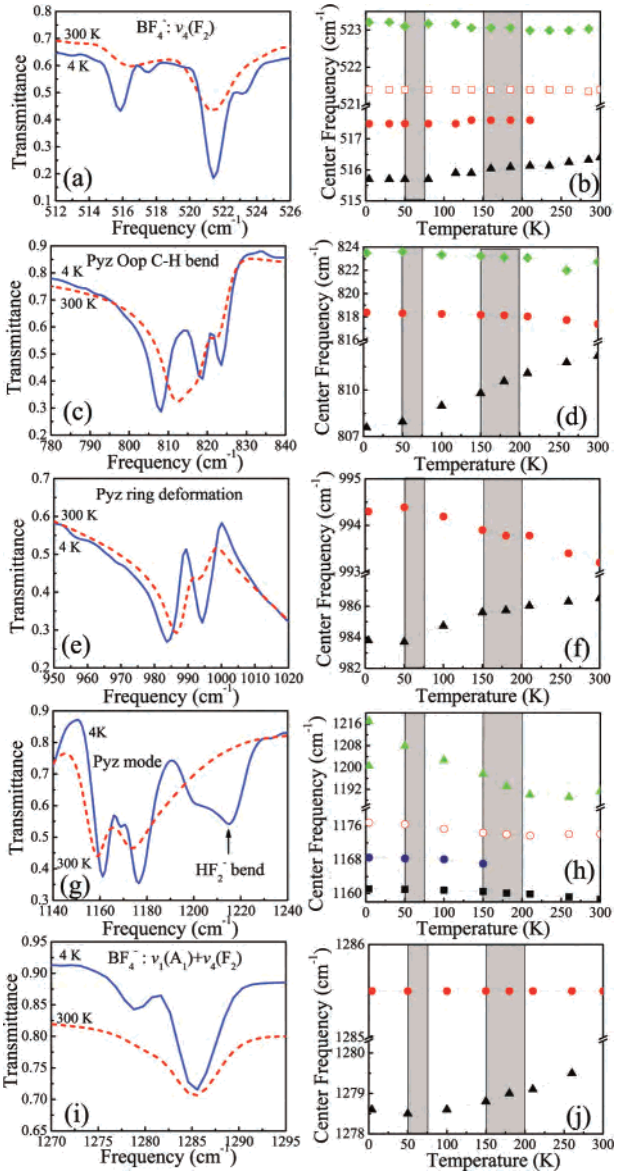

Figure 2. Close-up view of selected vibrational modes as observed in the transmittance spectrum of $Cu(HF_2)(pyz)_2BF_4$ at 300 and 4.2 K (left panels) and the corresponding mode frequencies as a function of the temperature for these features (right panels), highlighting the low-temperature mode softening and local structural distortions.

III. Results and Discussion

A. Low-Temperature Hydrogen Bonding and Structural Phase Transitions in $Cu(HF_2)(pyz)_2BF_4$. Figure 2 shows a close-up view of several characteristic vibrational modes of $Cu(HF_2)(pyz)_2BF_4$.[33] We assign the features centered near 522, 817, 986, 1217, and 1285 cm^{-1} to well-known BF_4^-, a pyrazine out-of-plane (Oop) C−H bend, pyrazine ring deformation, a HF_2^- bend, and BF_4^--related combination modes, respectively. These mode assignments were made by comparison with chemically similar model

(30) *SAINT*, version 6.28a ed.; Bruker AXS, Inc.: Madison, WI, 2001.
(31) Sheldrick, G. M. *SADABS*, version 2.03a ed.; Bruker AXS, Inc.: Madison, WI, 2001.
(32) Sheldrick, G. M. *SHELXTL*, version 6.12 ed.; Bruker AXS Inc.: Madison, WI, 2001.
(33) Spectroscopic work was performed on both single crystals and pressed-pellet samples of $Cu(HF_2)(pyz)_2BF_4$. The majority of the fundamental modes are saturated (below 3600 cm^{-1}) in single crystals.

compounds and with the aid of known functional group patterns.[34−38] Strikingly, many of these modes soften with decreasing temperature. To quantify these trends, we fit the spectra using standard peak-fitting techniques (right-hand panels, Figure 2).

The vibrational mode softening observed in $Cu(HF_2)(pyz)_2BF_4$ is interesting and unusual because vibrational modes generally harden with decreasing temperature.[39] Various pyrazine- and BF_4^--related structures show this trend most clearly. For instance, the 986 cm^{-1} pyrazine ring deformation mode (Figure 2e) and the 1420 cm^{-1} C−H in-plane bend (not shown) soften with decreasing temperature. At the same time, the position of the pyrazine-related out-of-plane C−H bend at 817 cm^{-1} (Figure 2c), the BF_4^- F_2 fundamental at 522 cm^{-1} (Figure 2a), and the related $F_2 + A_1$ combination mode at 1285 cm^{-1} (Figure 2i) are insensitive to temperature and do not show normal hardening behavior. Here and in Figure 2a,i, F_2 refers to the spectroscopic notation, not the F_2 molecule.[34] Several of the aforementioned pyrazine and BF_4^- modes in $Cu(HF_2)(pyz)_2BF_4$ split as well (Figure 2c,e,i), indicating a reduction in the local site symmetry with decreasing temperature. Spectral signatures of the bifluoride ligand have been studied by several authors.[34,37,40,41] The symmetric stretch resonates between 527 and 600 cm^{-1}, depending on the chemical nature of the counterion.[34,37,40,41] Further, it is Raman/infrared-active depending on the physical location of the H center with respect to the surrounding F centers. The fact that we do not see the bifluoride ion signature in our spectra between 527 and 600 cm^{-1} (Figure 3) indicates that the HF_2^- ligand is symmetric at all temperatures. The bending mode resonates between 1195 and 1233 cm^{-1}, depending on the coordination environment.[34,37,40,41] In $Cu(HF_2)(pyz)_2BF_4$, the HF_2^- bending mode (Figure 2g) appears as a broad shoulder at room temperature. It sharpens, splits slightly, and hardens by ~12 cm^{-1} at the base temperature. The asymmetric stretching mode of bifluoride, which has been observed between 1315 and 1730 cm^{-1}, unfortunately overlaps with strong pyrazine ring modes in $Cu(HF_2)(pyz)_2BF_4$, precluding analysis. Many other modes, including those at 135, 180, and 210 cm^{-1} (N−Cu−N) and 300 cm^{-1} (Cu−N stretching), also exhibit normal hardening behavior (Figure 3). No distortion of the Cu coordination environment is observed with decreasing temperature.

We attribute the anomalous mode softening in $Cu(HF_2)(pyz)_2BF_4$ to systematic changes in the hydrogen bonding between pyrazine H atoms and the F centers in BF_4^- and to a much lesser extent with HF_2^-. On the basis of the spectroscopic results in Figure 2, these interactions strengthen with decreasing temperature. These local changes in hydrogen-bonding interactions and the modified site symmetries drive weak second-order structural phase transitions near 150 and 50 K. This is consistent with our variable-temperature single-crystal X-ray diffraction analysis of $Cu(HF_2)(pyz)_2BF_4$, which shows a notable broadening of the diffraction peaks near 150 K.[26] These trends are replicated in the quasi-isostructural ClO_4^- analogue. Similar mode softening was also observed in two related model compounds: $Cu(pyz)_2(ClO_4)_2$ and $Cu(pyz)(NO_3)_2$.[25,28] Mode softening in the square antiferromagnet $Cu(pyz)_2(ClO_4)_2$ was attributed to enhanced low-temperature hydrogen-bonding interactions between the ClO_4^- counterion and pyrazine rings in the neighboring layer. The extensive interchain hydrogen-bonding interactions in 1D $Cu(pyz)(NO_3)_2$ are different. Here, nearly one-third of the total modes soften at low temperature, indicative of extensive interactions between the pyrazine rings and the nitrate groups.

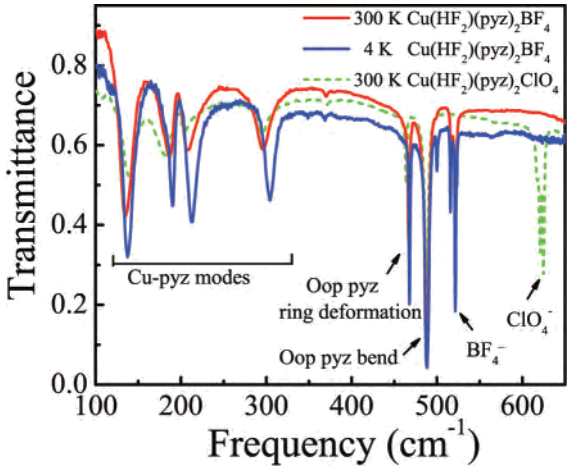

Figure 3. Transmittance spectra of $Cu(HF_2)(pyz)_2BF_4$ at 300 and 4.2 K along with the 300 K response of $Cu(HF_2)(pyz)_2ClO_4$. No stretching mode of the bifluoride bridging ligand is observed, indicating that HF_2^- is symmetric.

The available X-ray diffraction data are consistent with the anomalous vibrational mode softening in $Cu(HF_2)(pyz)_2BF_4$. Comparison of the local 300 K structure with that at 200 K shows that distances between the pyrazine ring H centers and the F centers associated with BF_4^- and HF_2^- decrease as the temperature is reduced. For instance, the distance between pyrazine H centers and the F centers on the BF_4^- anion decreases from 2.607 Å at 300 K to 2.564 Å at 200 K. At the same time, B−F and H−F bond lengths are elongated. These changes along with the simultaneous trend toward standard BF_4^- bond angles with decreasing temperature[42] facilitate improved hydrogen-bonding interactions with the bifluoride ligand. Strong H−F bonding is thus supported by an analysis of the structure. A summary of the crystallographic data is given in Table 1, and further details are available in the CIF file deposited as Supporting Information.[43]

B. Controlling the Hydrogen Bonding in $CuF_2(H_2O)_2(pyz)$: An Interesting Role for H_2O. Figure 4 shows a close-up view of several representative vibrational modes

(34) Nakamoto, K. *Infrared and Raman Spectra of Inorganic and Coordination Compounds*, 4th ed.; Wiley: New York, 1986.
(35) Hewett, K. B.; Shen, M.; Brummel, C. L.; Philips, L. A. *J. Chem. Phys.* **1994**, *100*, 4077.
(36) Bozio, R.; Meneghetti, M.; Pecile, C. *J. Chem. Phys.* **1982**, *76*, 5785.
(37) Harmon, K. M.; Lovelace, R. R. *J. Phys. Chem.* **1982**, *86*, 900.
(38) Dawson, P.; Hargreave, M. M.; Wilkinson, G. R. *Spectrochim. Acta* **1975**, *31A*, 1055.
(39) Bond lengths and important center-to-center distances in a crystalline lattice generally contrast at low temperature. Because $\omega \sim k/m^{1/2}$, vibrational mode frequencies generally harden with decreasing temperature.
(40) Ketelaar, J. A. A.; Vedder, W. *J. Chem. Phys.* **1951**, *19*, 654.
(41) Emsley, J. *Chem. Soc. Rev.* **1980**, *9*, 91.

Table 1. X-ray Crystallographic Data for $Cu(HF_2)(pyz)_2BF_4$ at 200 K

formula	$C_8H_9BCuF_6N_4$	space group	*P4/nbm* (No. 125)
a (Å)	9.6872(6)	*T* (K)	200(2)
c (Å)	6.5998(7)	ρ_{calc} (g cm^{-3})	1.874
V (Å^3)	619.34(9)	μ (mm^{-1})	1.832
Z	2	$R(F_o)^a$	0.0533
fw	349.54	$R_w(F_o^2)^b$	0.1492

^{a} $R(F_o) = \sum||F_o| - |F_c||/\sum|F_o|$ ($I > 2\sigma$). ^{b} $R_w(F_o^2) = [\sum w(|F_o^2| - |F_c^2|)^2/\sum wF_o^2]^{1/2}$ (all data).

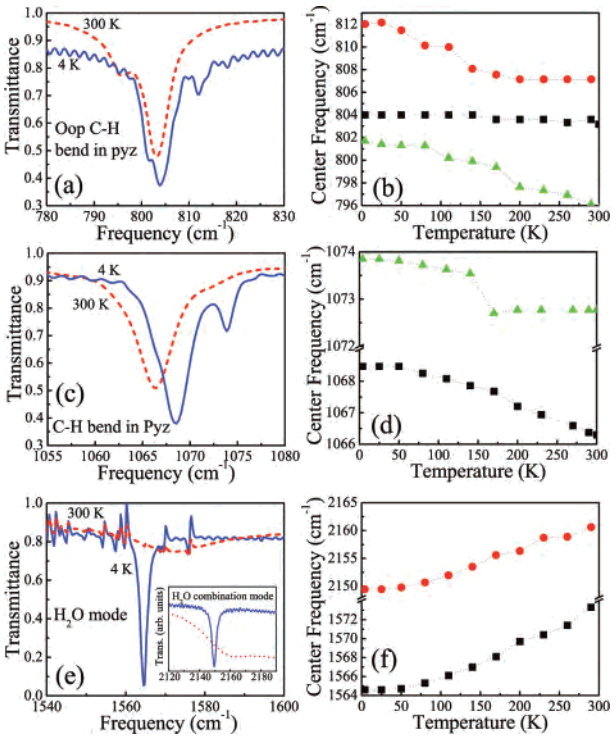

Figure 4. Close-up view of selected modes in the temperature-dependent transmittance spectrum of $CuF_2(H_2O)_2(pyz)$ (left panels) and corresponding mode frequencies of these features as a function of the temperature (right panels), highlighting the low-temperature mode softening.

of 1D $CuF_2(H_2O)_2(pyz)$ along with a peak-fitting analysis of each structure. The features near 803, 1067, and 1565 cm^{-1} are assigned as out-of-plane C−H bending that deforms the pyrazine ring, C−H bending of the pyrazine ring, and H_2O bending, respectively. In most instances in which a material contains coordinated H_2O molecules of crystallization, the lattice H_2O has a bending mode between 1600 and 1650 cm^{-1}.[34,44] In $CuF_2(H_2O)_2(pyz)$, however, the H_2O bending mode resonates at a significantly lower frequency, indicating a severe distortion of the local structure and chemical environment. In fact, its resonance near 1573 cm^{-1} at 300 K and 1565 cm^{-1} at 4 K in $CuF_2(H_2O)_2(pyz)$ is more akin to that found for gaseous H_2O (at 1595 cm^{-1}).[45] The peak near 2150 cm^{-1} (inset, Figure 4e) is assigned as a combination mode. It derives from a combination of the aforementioned H_2O bending mode and vibrational motion

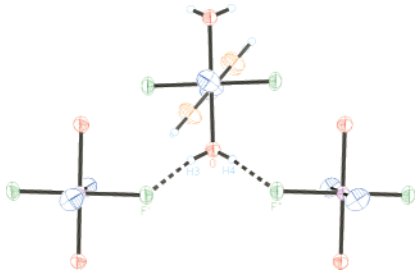

Figure 5. Close-up view of the coordination environment around H_2O in $CuF_2(H_2O)_2(pyz)$.

near 619 cm^{-1}.[35,44] This feature is also severely red-shifted compared to its position in other hydrated materials.[34,44] Note that the temperature dependences of the fundamental and combination modes are similar (Figure 4f).

The most striking trends with temperature in $CuF_2(H_2O)_2$-(pyz) pertain to the H_2O-related modes at 1565 and 2150 cm^{-1} (Figure 4e). Between 300 and 4 K, the fundamental mode red-shifts by ∼9 cm^{-1} and the combination mode red-shifts by ∼11 cm^{-1}. The behavior of pyrazine-related modes is different. Several are relatively insensitive to temperature. These include features at 803 (Figure 4a), 1150, and 1419 cm^{-1}. Others exhibit a normal hardening trend. These include structures near 1067 cm^{-1} (Figure 4c) and the ring deformation mode near 1167 cm^{-1}. These frequency shifts occur gradually over the full temperature range of our investigation.

We attribute the aforementioned softening of the H_2O bending mode in $CuF_2(H_2O)_2(pyz)$ to improved low-temperature hydrogen bonding between H and F centers. At the same time, the behavior of selected pyrazine modes is consistent with a modestly improved interaction between pyrazine H atoms and the fluoride ligand at 4 K. Splitting of the pyrazine modes (Figure 4a,c) is very clear at low temperature but is probably also present as a weak shoulder at 300 K, indicating that the hydrogen-bonding network may locally distort the pyrazine building-block molecule. Even in the presence of strong low-temperature hydrogen-bonding interactions, no clear structural phase transition is observed. This is because both local site symmetry and macroscopic crystal symmetry are retained over the temperature range of our investigation despite modification to individual bond lengths and angles.

Complementary X-ray diffraction data at 300, 150, and 20 K verify these findings.[26] With decreasing temperature, a significant increase in the O−H bond length is observed, and the H_2O bond angle (Figure 5) widens slightly to facilitate hydrogen bonding with nearby F centers. At the same time, H···F distances decrease from 1.864/1.844 Å at 300 K to 1.810/1.794 Å at 20 K.[46] Distortion of the H_2O molecule embedded in the lattice is consistent with both the unusual resonance frequency of the fundamental H_2O bending mode in $CuF_2(H_2O)_2(pyz)$ and the observed red shift of this feature and its associated combination mode with

(42) The F−B−F bond angles go from 105.63°/117.47° at 300 K to 106.39°/115.83° at 200 K.

(43) Although a full complement of single-crystal structural data was collected, the structure could not be solved below 200 K because the crystal breaks into multiple domains.

(44) Brubach, J. B.; Mermet, A.; Filabozzi, A.; Gerschel, A.; Roy, P. *J. Chem.* **2005**, *122*, 184509.

(45) Bernath, P. F. *Phys. Chem. Chem. Phys.* **2002**, *4*, 1501.

(46) The geometry of the H_2O molecule was constrained during structural refinement, and these H···F distances are therefore only approximate. However, the trend on cooling is clear. A more accurate determination of the location of the H atoms would require neutron diffraction, which is beyond the scope of this paper.

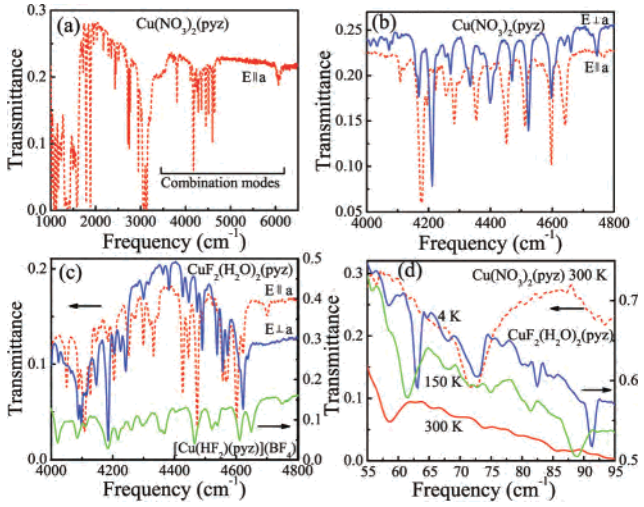

Figure 6. (a) 300 K polarized transmittance spectrum of $Cu(pyz)(NO_3)_2$ parallel to the magnetic chain (*a* axis) direction. (b) Close-up view of the combination mode region indicated in panel a, showing both $\vec{E}||a$ and $\vec{E}\perp a$ polarizations. (c) Close-up view of the 300 K transmittance spectra of $Cu(HF_2)(pyz)_2BF_4$ compared with that of $CuF_2(H_2O)_2(pyz)$. (d) Variable-temperature far-infrared transmittance spectra of $CuF_2(H_2O)_2(pyz)$ compared to the 300 K response of the $Cu(pyz)(NO_3)_2$ model compound.

decreasing temperature (Figure 4e). For instance, the short 300 K O···F distances [2.6051(12)/2.6176(11) Å] are indicative of hydrogen bonding; they decrease to 2.5965(20)/2.6121(19) Å at 20 K. Other angles and important center-to-center distances also change with temperature.[26] Because the dominant pyrazine-related magnetic exchange pathways in $CuF_2(H_2O)_2(pyz)$ are likely to be mediated by the F···H−O hydrogen-bonding network, we conclude that this network gets stronger with decreasing temperature. Interestingly, low-temperature long-range ordering was recently discovered.[26]

C. Evidence for Multiphonon Structure in Low-Dimensional Polymeric Magnets. Figure 6a displays the vibrational response of $Cu(NO_3)_2(pyz)$ polarized along the magnetic chain direction. This compound is the prototype in the family of pyrazine-based polymeric magnets. Previous dynamics studies[28] focused primarily on the unusual low-temperature hydrogen bonding. A detailed understanding of the striking set of high-energy vibrational features centered at ∼4400, 6000, and 9000 cm^{-1} was unfortunately missing. The availability of this family of chemically related low-dimensional polymeric magnets has allowed us to reexamine this problem. The finding that multiphonon structure dominates the high-energy vibrational response of $Cu(NO_3)_2(pyz)$, $CuF_2(H_2O)_2(pyz)$, and $Cu(HF_2)(pyz)_2BF_4$ has implications for understanding the dynamics of other magnetic solids.

Figure 6b displays a close-up view of the unusual vibrational structure near 4400 cm^{-1} in $Cu(NO_3)_2(pyz)$. Strikingly similar features appear in the response of $CuF_2(H_2O)_2(pyz)$ and $Cu(HF_2)(pyz)_2BF_4$ (Figure 6c). Because the chemical building blocks of these materials (pyrazine, HF_2, and BF_4) have no fundamental vibrational modes above 3200 cm^{-1}, these complex bands must be due to combinations of intense fundamentals. Previous infrared and Raman work on molecular pyrazine provides several candidates for such a two-photon process,[47] and in a related study, a series of C−H stretching mode overtones have been implicated in liquid isoxazole, thiazole, and related dimethyl derivatives.[48] On the basis of these studies, we propose that the multiphonon structure centered near 4400 cm^{-1} in these low-dimensional polymeric magnets arises from the combination of infrared-active B_{1u} and B_{2u} C−H stretching modes near 3100 cm^{-1} and Raman-active A_g modes near ∼1016, 1233, and 1580 cm^{-1}. The totally symmetric A_g modes near ∼1016, 1233, and 1580 cm^{-1} are related to pyrazine ring deformation, C−H bending, and C−C stretching, respectively.[47] They are reported to be among the most intense of all Raman-active modes in pyrazine. According to group theoretical analysis, the combination of A_g and B_{1u}/B_{2u} modes is symmetry-allowed. In other words, the direct product of $A_g\otimes\mu\otimes B_{1u}$ and $A_g\otimes\mu\otimes B_{2u}$ contains A_g. Here, μ is the moment operator.

We can explain multiphonon character of the vibrational response near 4400 cm^{-1} in $Cu(NO_3)_2(pyz)$ by invoking strong coupling, but what about the fine structure (Figure 6b)? Based on the energy scale of this splitting, which ranges from 50 to 110 cm^{-1} in $Cu(NO_3)_2(pyz)$, the combination modes that derive from infrared-active C−H stretching and Raman-active A_g modes of pyrazine also mix with low-frequency lattice vibrations to yield the complex structure observed in the spectra. In principle, one (or more) lattice mode(s) may be involved in the coupling process, although the irregular nature of the fine structure is consistent with the participation of multiple modes. Direct measurement of the far-infrared lattice response in $Cu(pyz)(NO_3)_2$ (Figure 6d) shows several interesting candidates. Clear lattice modes are observed at ∼51, 72, and 95 cm^{-1} in the 300 K spectrum, in excellent agreement with the energy scale of the aforementioned splitting. $Cu(HF_2)(pyz)_2BF_4$ and $CuF_2(H_2O)_2(pyz)$ also show complex multiphonon behavior near 4400 cm^{-1} (Figure 6c). The characteristic energy of the fine structure is similar to that already discussed for the model compound (between 50 and 110 cm^{-1} in $Cu(HF_2)(pyz)_2BF_4$ and from 35 to 70 cm^{-1} in $CuF_2(H_2O)_2(pyz)$). Direct measurement of the far-infrared response of $CuF_2(H_2O)_2(pyz)$ shows features at ∼58, 63, 72, 82, and 92 cm^{-1} in the 4 K spectrum (Figure 6d).[49] The modes near 63, 82, and 92 cm^{-1} are associated with pyrazine motion and harden with decreasing temperature.[47,50] The H_2O-related lattice mode near 72 cm^{-1} softens with decreasing temperature. All of these modes are polarization-independent. Slight differences in the lattice response account for subtle differences in the multiphonon structures of these compounds.

This family of polymeric magnets also has a series of unusual vibrational modes centered near 6000 and 9000 cm^{-1}. These features were first noticed in $Cu(NO_3)_2(pyz)$,[28] although no detailed explanation was given. On the basis of our understanding of the multiphonon modes near 4000 cm^{-1} and the strong mixing implied by such an assignment, we attribute the structures near 6000 and 9000 cm^{-1} to a series

(47) Sbrana, G.; Schettino, V.; Righini, R. *J. Chem. Phys.* **1973**, *59*, 2441.
(48) Sbrana, G.; Miranda, M. M. *J. Phys. Chem. A* **1998**, *102*, 7603.
(49) Size and thickness considerations prevented far-infrared studies of $Cu(HF_2)(pyz)_2BF_4$.
(50) Ito, M.; Shigeoka, T. *J. Chem. Phys.* **1966**, *44*, 1001.

of overtones that derive from C−H stretching modes. These two- and three-phonon modes can be (i) a combination of infrared-active C−H stretching modes or (ii) a combination of both infrared- and Raman-active C−H stretching modes. Infrared modes near 3100 cm^{-1} and Raman-active features near 3054 cm^{-1} are likely candidates for this coupling. Similar overtones have been observed in liquid isoxazole, thiazole, and related dimethyl derivatives.[48] Overtones of metal−oxygen stretching modes have also been employed to track subtle changes in hydrogen bonding in $VOHPO_4 \cdot {}^1/_2H_2O$.[12]

IV. Conclusion

We report a systematic investigation of the temperature-dependent infrared vibrational spectra of a family of chemically related coordination polymer magnets. We focus on the response of $Cu(HF_2)(pyz)_2BF_4$ and $CuF_2(H_2O)_2(pyz)$, comparing the results with prototypes such as $Cu(NO_3)_2(pyz)$. Anomalous mode softening is observed throughout the temperature range of investigation, a result that we attribute to enhanced low-temperature hydrogen bonding. In $Cu(HF_2)(pyz)_2BF_4$, the improved hydrogen bonding drives two weak local structural distortions. The striking multiphonon effects in these materials derive from coupling of an infrared-active fundamental mode with strong Raman-active modes of appropriate symmetry that derive from pyrazine motion. On the basis of the spectroscopic evidence, these interactions are ubiquitous to this family of coordination polymers and work to stabilize the low-temperature long-range magnetic order. Similar interactions are likely to be present in other molecule-based magnets.

Acknowledgment. Research at the University of Tennessee was supported by the Materials Science Division, Office of Basic Energy Sciences, at the U.S. Department of Energy under Grant DE-FG02-01ER45885. Work at Eastern Washington University was supported by an award from the Research Corporation. Work at Argonne National Laboratory was supported by the Office of Basic Energy Sciences, Division of Materials Science, U.S. Department of Energy, under Contract DE-AC02-06CH11357.

Supporting Information Available: Further structural details on $Cu(HF_2)(pyz)_2BF_4$ in CIF format. This material is available free of charge via the Internet at http://pubs.acs.org.

IC070122T